Scoping Analysis on Energy Release and Core Explosion in CDA of PGSFR using CDA-ER and CDA-CEME Codes

Seung Won Lee[*], Seok Hun Kang, Soo-Dong Suk, Kwi-Seok Ha
Fast Reactor Design Division
Korea Atomic Energy Research Institute (KAERI)
Daedeok-daero 989-111, Yuseong-gu, Daejeon, 305-353, Republic of Korea
[*]*Corresponding author: swonlee@kaeri.re.kr*

1. Introduction

The severe accident is accident condition more severe than a design basis accident and involving significant core degradation are termed severe accidents by International Atomic Energy Agency (IAEA) [1]. Also, the severe accident is a type of accident that may challenge safety systems at a level much higher than expected by Nuclear Regulatory Commission (NRC) [2]. By French Institute for Radiological protection and Nuclear Safety (IRSN), the severe accident refers to an event causing significant damage to reactor fuel and resulting from more or less complete core meltdown [3].

In general, the severe accident is classified by three phases. The first phase is the initiation (pre-disassembly) phase that occurs the gradual core meltdown from accident initiation to the point of neutronic shutdown with an intact geometry. The second phase is the transition phase that happens the fuel transition from a solid to a liquid phase. Fuel and cladding can melt to form a molten pool and core can boil, then criticality conditions can recur. The third phase is the disassembly phase. In other words, this phase is Core Disruptive Accident (CDA). Power excursion is followed until the core is disassembled in this phase. In the early considerations of Liquid Metal Fast Breeder Reactor (LMFBR) energetics, the term Hypothetical Core Disruptive Accidents (HCDAs) was in common use. This was not only to connote the extremely low probability of initiation of such accidents, but also the tentative nature of our understanding of their behavior and resulting consequences. Certain hypothetical situations were postulated for the purpose of analytically realizing an energetic behavior and thus attempting to establish "bounds of severity." After nearly twenty years of intensive research and development, it appears that there is no longer reason to resort to such examinations of hypothetical circumstances [4].

Classically, CDA is analyzed in three phases. In the first phase, the source term is defined in the form of a core bubble, which is a two-phase mixture of fuel structural materials and coolant, having the potential to release a specified quantity of mechanical energy. In the second phase, the mechanical consequences, such as straining in the vessels, impact on the top shield, and sodium release into the Reactor Containment Building (RCB), are analyzed. In the third phase, the post-accident heat removal aspect is analyzed.

Whether CDA are potentially real events that must be considered in establishing design bases for the containment, very low probability events that can be eliminated from design basis considerations, or mechanistically unrealistic fantasies of creative analysts has been hotly debated. The answer may be design dependent [5]. An argument has been made by advocates of metallic-fueled SFR designs that in scenarios of interest, fuel melting within a fuel pin results in an axial movement that decreases reactivity, fuel failure when it occurs w ould likely be above the active core region, and that the fuel debris would be swept out of the core region. This removal of fuel from the core will most likely shut down the reactor before fuel vaporization becomes a possibility [6].

A numerical analysis is conducted to estimate the energy release and core expansion behavior induced by CDA in Sodium-cooled Fast Reactor (SFR). An analysis of the CDA energy release based on the Bethe-Tait method [7] is carried out and its results are used as the initial conditions for the core explosion computations. Calculations are made for the super prompt power excursions of a Prototype Gen-IV SFR (PGSFR) core and the influences of the Doppler effect on the power excursions are investigated. The transient pressure and temperature of the core are examined by solving the equation of state of ideal gas and nonlinear governing equation of momentum conservation in one-dimensional spherical coordinates. Energy balance is examined during the core expansion process [8].

2. Modeling for Analyzing CDA of PGSFR

Calculations have been performed for analyzing CDA of PGSFR which is a 150 MWe pool type SFR and use metallic fuel, U-10Zr. The PGSFR core is designed to generate 392.1 MWth of power as shown in Fig. 1 [9]. The core consists of 52 inner core Fuel Assemblies (FAs), 60 outer core FAs, 6 primary control rods, 3 secondary control rods, 90 reflector assemblies and 102 B_4C shield assemblies. Inner and outer core assemblies include 217 fuel pins containing a metal fuel slug of U-10Zr in columns.
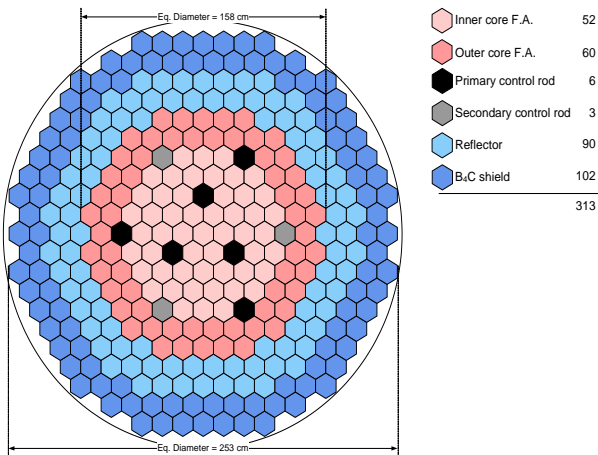
Fig. 1. Core configuration of PGSFR [9].

Table I [9, 10] shows the calculation parameters used in the scoping analysis about CDA of PGSFR and reactor core characteristic. The specific power of fuel is 52,012.65 W/kg, the neutron lifetime is $3.29 \cdot 10^{-7}$ s, the delayed neutron fraction is 0.0067, the fuel mass containing only U is 7,538.55 kg, the density of solid fuel is 15,900 kg/m^3, the radius of spherical core is 0.79 m and the vessel radius is 4.277 m.

Table I : Calculation Parameters and Core Characteristic [9, 10]

Net plant power	150 MWe / 392.1 MWth
Net plant efficiency	38.25 %
Specific power of fuel	52,012.65 W/kg
Enrichment	19.2 %
Reactor type	Pool
Core configuration	Radially heterogeneous
Active core height	900 mm
Core diameter	2,530 mm
Assembly pitch	136.36 mm
Fuel form	U-10Zr
Fuel pins per assembly	217
Inlet / Outlet temperature	390 / 545 ℃
Fuel burnup	66.1 GWd/MT (74.2 / 57.2)
Neutron lifetime	$3.29 \cdot 10^{-7}$ s
Delayed neutron fraction	0.0067
Fuel mass	7,538.55 kg
Density of solid fuel	15,900 kg/m^3
Radius of spherical core	0.79 m
Vessel Radius	4.277 m

Fig. 2 shows the CDA scenario: Sodium coolant drains out or boils away from the core, fuel from the middle of the core melt and trickle down, molten fuel is located into the lower part of the core and is retained there, the upper portion of the core is assumed to fall by gravity, the reactivity increases above prompt critical at the insertion rate and strong explosion is occurred and terminated by disassembly of the core. The CDA is

assumed in the three cases: when all inner cores (52/52) were melted, when all inner cores (52/52) and half of outer cores (30/60) were melted and when whole cores were melted. Table II [11] shows molten fuel mass, reactivity insertion, reactivity insertion rate and delayed neutron fraction in each accident conditions. The reactivity insertion rate is calculated using the height and time from active fuel region to lower part of the core as shown in Fig. 3 [10].
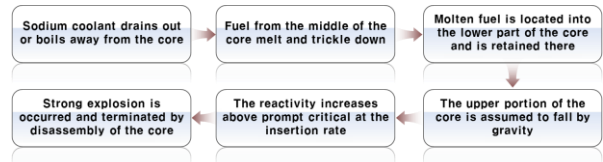

Fig. 2. CDA scenario.

Table II : Molten Fuel Mass, Reactivity Insertion, Reactivity Insertion Rate and Delayed Neutron Fraction in Each Accident Conditions [11]

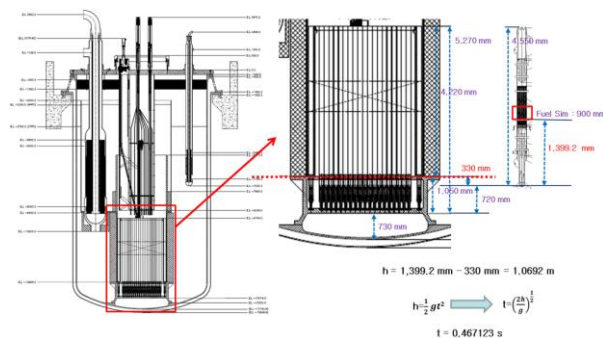|	Inner core (52/52)	Inner core (52/52) + Outer core (30/60)	Whole core (52/52 + 60/60)
Molten fuel mass (kg)	3500.04	5519.30	7538.55
Reactivity insertion ($)	29.18 ±0.45 (29.63[*])	35.64 ±0.47 (36.11[*])	39.25 ±0.47 (39.72[*])
Reactivity insertion rate ($/s)	63.43	77.30	85.03
Delayed neutron fraction	0.00713 ±0.00011 (0.00702[*])	0.00716 ±0.00013 (0.00703[*])	0.00695 ±0.00013 (0.00682[*])

[*] : the conservative value

Fig. 3. Height and time from active fuel region to lower part of the core [10].

The reactivity insertion and time that the upper portion of the core is assumed to fall by gravity are calculated conservatively. So, the calculated reactivity insertion rate is conservative. Also, the delayed neutron fraction is used conservatively.

3. Analysis Results

3.1 Energy Release and Pressure Behavior using CDA-ER Code

A numerical analysis was conducted to estimate the energy release and pressure behavior induced by CDA in PGSFR. A numerical code, CDA-Energy Release (ER), which is based on the Bethe-Tait method was developed to calculate the energy release and pressure during CDA. The influences of Doppler effect on the power excursions were also estimated [12].

It was assumed in the Bethe-Tait method that the power distribution of reactivity worth was independent of time and the reactivity changes were obtained using the first order perturbation theory. The density of molten core material was assumed to be constant in the hydrodynamic equations describing the equation of state of the molten core. Thus, the propagation and reflection of pressure wave were ignored. The power excursion was divided into two phases in the method. Reactivity was added at a constant rate and the power increased during the first phase. The reactivity effect coming from material movement was incorporated, but any further addition of reactivity was neglected during the second phase. The reactivity feedback from Doppler effect, which was ignored in the Bethe-Tait method, is added during the second phase calculation of this work [8].

Fig. 4 shows the calculated results of energy release and pressure behavior induced by CDA without Doppler effect in PGSFR when all inner cores were melted. The reactivity insertion rate of this situation is 63.43 $/s. The analyzed maximum energy release and pressure were 3.33 GJ and 4.04 GPa, respectively. Fig. 5 shows the calculated results of energy release and pressure behavior induced by CDA with Doppler effect in PGSFR when all inner cores were melted (63.43 $/s). The analyzed maximum energy release and pressure were 2.76 GJ and 2.54 GPa, respectively. When Doppler effect is considered in this situation, 17.12 % of the maximum energy release and 37.13 % of the maximum pressure are decreased.
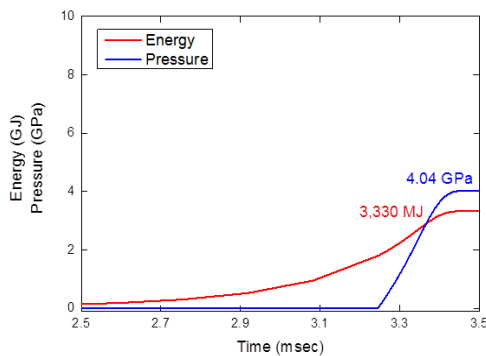

Fig. 4. Energy release and pressure behavior induced by CDA without Doppler effect in PGSFR when all inner cores were melted (63.43 $/s).

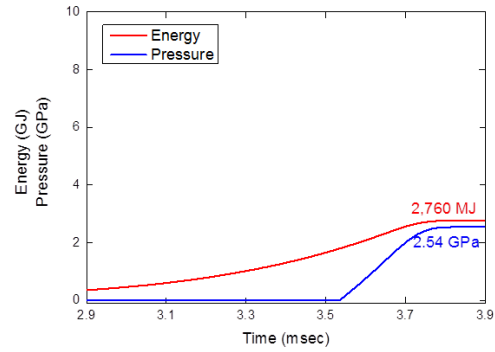Fig. 5. Energy release and pressure behavior induced by CDA with Doppler effect in PGSFR when all inner cores were melted (63.43 $/s).

Fig. 6 shows the calculated results of energy release and pressure behavior induced by CDA without Doppler effect in PGSFR when all inner cores and half of outer cores were melted. The reactivity insertion rate of this situation is 77.30 $/s. The analyzed maximum energy release and pressure were 5.45 GJ and 4.36 GPa, respectively. Fig. 7 shows the calculated results of energy release and pressure behavior induced by CDA with Doppler effect in PGSFR when all inner cores and half of outer cores were melted (77.30 $/s). The analyzed maximum energy release and pressure were 4.59 GJ and 2.93 GPa, respectively. When Doppler effect is considered in this situation, 15.78 % of the maximum energy release and 32.80 % of the maximum pressure are decreased.
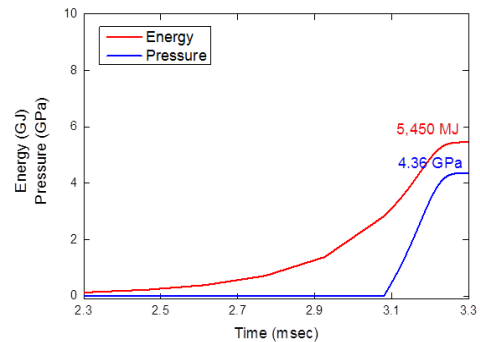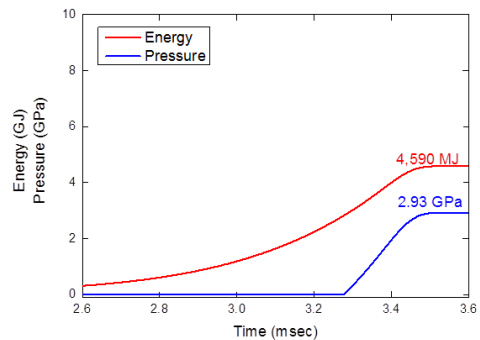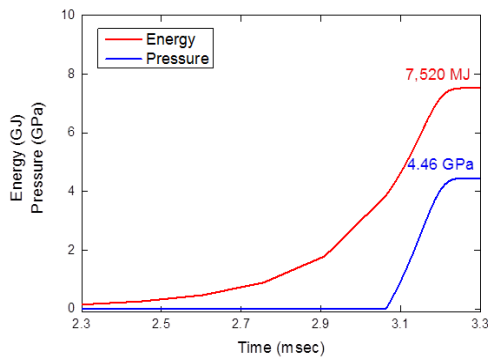

Fig. 6. Energy release and pressure behavior induced by CDA without Doppler effect in PGSFR when all inner cores and half of outer cores were melted (77.30 $/s).

Fig. 7. Energy release and pressure behavior induced by CDA with Doppler effect in PGSFR when all inner cores and half of outer cores were melted (77.30 $/s).

Fig. 8 shows the calculated results of energy release and pressure behavior induced by CDA without Doppler effect in PGSFR when whole cores were melted. The reactivity insertion rate of this situation is 85.03 $/s. The analyzed maximum energy release and pressure were 7.52 GJ and 4.46 GPa, respectively. Fig. 9 shows the calculated results of energy release and pressure behavior induced by CDA with Doppler effect in PGSFR when whole cores were melted (85.03 $/s). The analyzed maximum energy release and pressure were 6.38 GJ and 3.06 GPa, respectively. When Doppler effect is considered in this situation, 15.16 % of the maximum energy release and 31.39 % of the maximum pressure are decreased.

Fig. 8. Energy release and pressure behavior induced by CDA without Doppler effect in PGSFR when whole cores were melted (85.03 $/s).
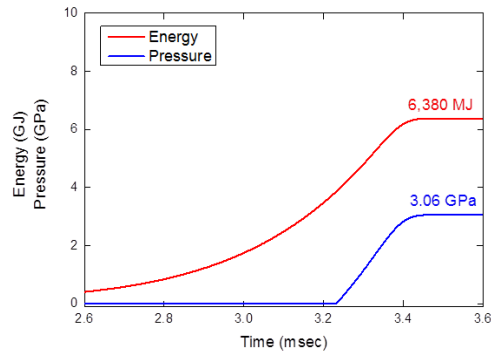

Fig. 9. Energy release and pressure behavior induced by CDA with Doppler effect in PGSFR when whole cores were melted (85.03 $/s).

Fig. 10 shows the calculated results of energy release and pressure behavior induced by CDA without Doppler effect in PGSFR when whole cores were melted. The reactivity insertion rate of this situation is 100 $/s conservatively. The analyzed maximum energy release and pressure were 7.80 GJ and 4.79 GPa, respectively. Fig. 11 shows the calculated results of energy release and pressure behavior induced by CDA with Doppler effect in PGSFR when whole cores were melted (100 $/s). The analyzed maximum energy release and pressure were 6.65 GJ and 3.39 GPa, respectively. When Doppler effect is considered in this situation,

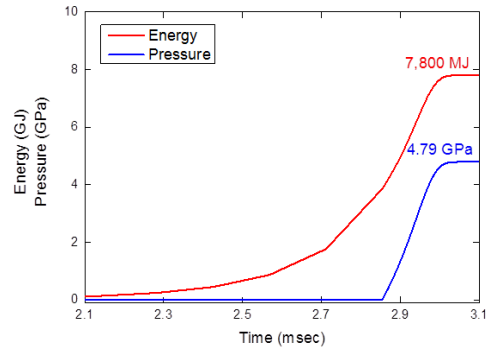14.74 % of the maximum energy release and 29.23 % of the maximum pressure are decreased.

Fig. 10. Energy release and pressure behavior induced by CDA without Doppler effect in PGSFR when whole cores were melted (conservatively 100 $/s).
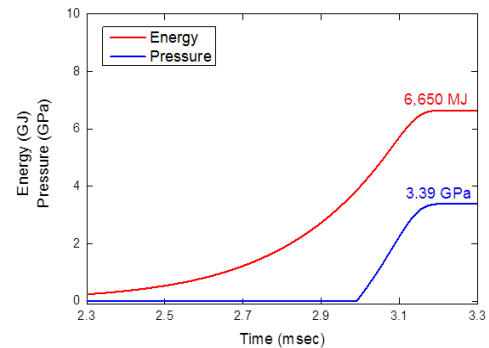

Fig. 11. Energy release and pressure behavior induced by CDA with Doppler effect in PGSFR when whole cores were melted (conservatively 100 $/s).

The significant influences of Doppler effect on the power excursions are observed. Energy release and pressure rises are significantly reduced as shown in Figs. 4 through 11.

3.2 Mechanical Energy using CDA-CEME Code

In a nuclear explosion, the energy is produced as a result of the formation of different atomic nuclei by the redistribution of the protons and neutrons within the interacting nuclei. The sudden energy release causes a considerable increase of temperature and pressure so that all the materials are converted into hot and compressed gases. Since these gases are at very high temperatures and pressures, they emit a shock wave into the surrounding medium. It is known that the shock wave propagating into the medium contains about half of the explosion energy in an underwater explosion [13]. The remainder resides as both kinetic energy associated with the expansion of a gaseous bubble of reaction products, and as internal energy (heat) within the explosion products themselves. The shock wave continues to travel away carrying with it about one-fourth of the original explosion energy. Therefore, the initial high pressure and energy in the gas sphere are considerably reduced after the shock wave emission,

which is not evaluated in present calculations, and the nuclear explosion leaves about 40% of its energy behind as the initial bubble energy [14, 15].

Hydrodynamic and thermodynamic computations are performed using the code developed, CDA-Core Explosion Mechanical Energy (CEME) in this work for the simulated CDA's condition. The transient pressure, temperature, and expansion of the core bubble are calculated through solving the equation of the state of ideal gas and the nonlinear governing equation of the momentum conservation in one-dimensional spherical coordinates. The core is treated as an adiabatic homogeneous ideal gas but the inertial effects of the gas are ignored in the calculation. The motion of a spherical explosion bubble oscillating in an incompressible homogeneous inviscid fluid are numerically computed using an ideal gas model for the behavior of the bubble interior [16].
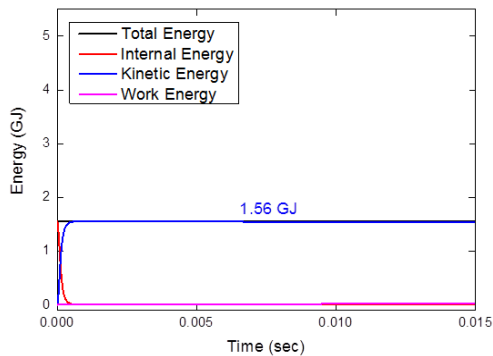

Fig. 12. Energy distributions during 0.015 seconds after the explosion without Doppler effect in PGSFR when all inner cores were melted (63.43 $/s).
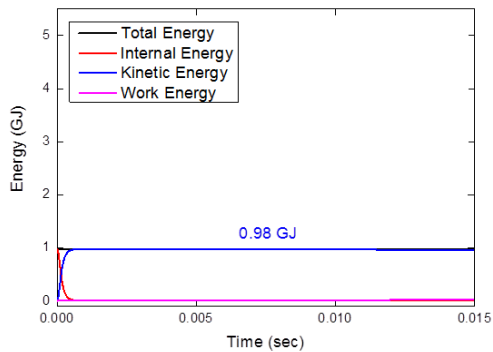

Fig. 13. Energy distributions during 0.015 seconds after the explosion with Doppler effect in PGSFR when all inner cores were melted (63.43 $/s).

Fig. 12 shows the calculated results of the energy distributions during 0.015 seconds after the explosion without Doppler effect in PGSFR when all inner cores were melted. The reactivity insertion rate of this situation is 63.43 $/s. The total energy is calculated to be 1.56 GJ. At 0.01 s, the kinetic energy of the sodium is 1.54 GJ, while the expansion work and internal energy of the bubble are 17.6 MJ and 1.45 J, respectively. Fig. 13 shows the calculated results of the energy distributions during 0.015 seconds after the explosion with Doppler

effect in PGSFR when all inner cores were melted (63.43 $/s). The total energy is calculated to be 0.98 GJ. At 0.01 s, the kinetic energy of the sodium is 0.97 GJ, while the expansion work and internal energy of the bubble are 13.4 MJ and 3.86 J, respectively.

Fig. 14 shows the calculated results of the energy distributions during 0.015 seconds after the explosion without Doppler effect in PGSFR when all inner cores and half of outer cores were melted. The reactivity insertion rate of this situation is 77.30 $/s. The total energy is calculated to be 1.68 GJ. At 0.01 s, the kinetic energy of the sodium is 1.66 GJ, while the expansion work and internal energy of the bubble are 18.5 MJ and 1.23 J, respectively. Fig. 15 shows the calculated results of the energy distributions during 0.015 seconds after the explosion with Doppler effect in PGSFR when all inner cores and half of outer cores were melted (77.30 $/s). The total energy is calculated to be 1.13 GJ. At 0.01 s, the kinetic energy of the sodium is 1.12 GJ, while the expansion work and internal energy of the bubble are 14.6 MJ and 2.86 J, respectively.
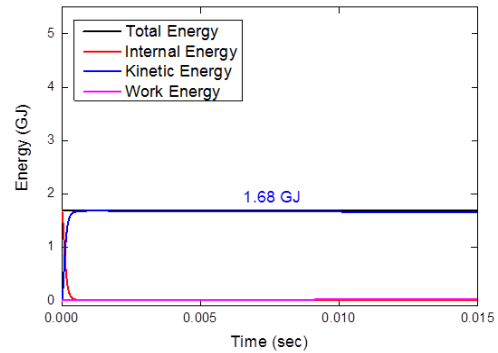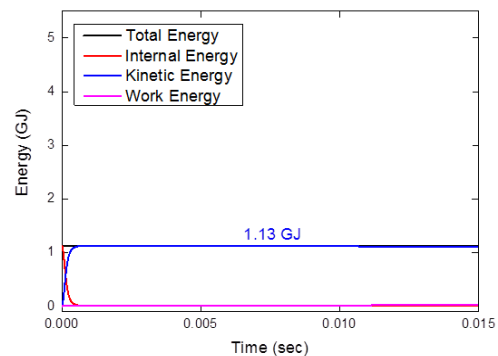

Fig. 14. Energy distributions during 0.015 seconds after the explosion without Doppler effect in PGSFR when all inner cores and half of outer cores were melted (77.30 $/s).

Fig. 15. Energy distributions during 0.015 seconds after the explosion with Doppler effect in PGSFR when all inner cores and half of outer cores were melted (77.30 $/s).

Fig. 16 shows the calculated results of the energy distributions during 0.015 seconds after the explosion without Doppler effect in PGSFR when whole cores were melted. The reactivity insertion rate of this situation is 85.03 $/s. The total energy is calculated to be 1.72 GJ. At 0.01 s, the kinetic energy of the sodium is 1.70 GJ, while the expansion work and internal energy of the

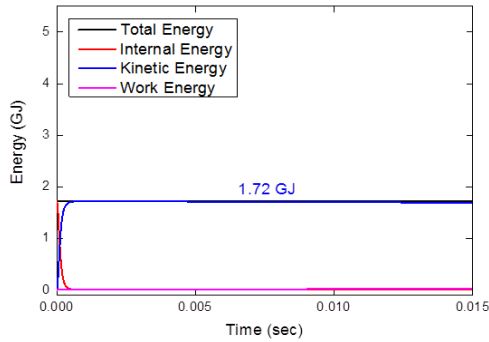bubble are 18.7 MJ and 1.17 J, respectively. Fig. 17 shows the calculated results of the energy distributions during 0.015 seconds after the explosion with Doppler effect in PGSFR when whole cores were melted (85.03 $/s). The total energy is calculated to be 1.18 GJ. At 0.01 s, the kinetic energy of the sodium is 1.17 GJ, while the expansion work and internal energy of the bubble are 14.9 MJ and 2.61 J, respectively.

Fig. 16. Energy distributions during 0.015 seconds after the explosion without Doppler effect in PGSFR when whole cores were melted (85.03 $/s).
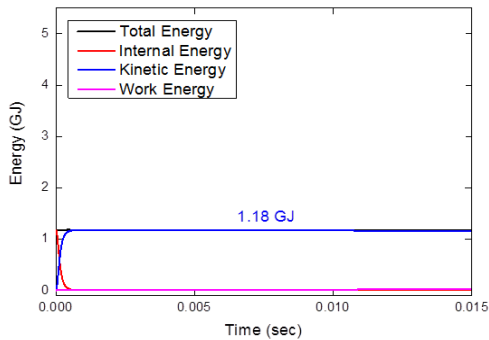

Fig. 17. Energy distributions during 0.015 seconds after the explosion with Doppler effect in PGSFR when whole cores were melted (85.03 $/s).

Fig. 18 shows the calculated results of the energy distributions during 0.015 seconds after the explosion without Doppler effect in PGSFR when whole cores were melted. The reactivity insertion rate of this situation is 100 $/s conservatively. The total energy is calculated to be 1.85 GJ. At 0.01 s, the kinetic energy of the sodium is 1.83 GJ, while the expansion work and internal energy of the bubble are 19.5 MJ and 1.01 J, respectively. Fig. 19 shows the calculated results of the energy distributions during 0.015 seconds after the explosion with Doppler effect in PGSFR when whole cores were melted (100 $/s). The total energy is calculated to be 1.31 GJ. At 0.01 s, the kinetic energy of the sodium is 1.29 GJ, while the expansion work and internal energy of the bubble are 15.9 MJ and 2.10 J, respectively.
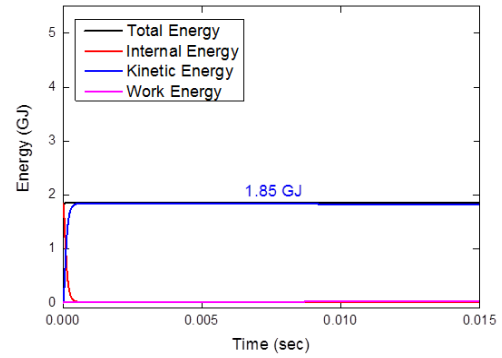

Fig. 18. Energy distributions during 0.015 seconds after the explosion without Doppler effect in PGSFR when whole cores were melted (conservatively 100 $/s).
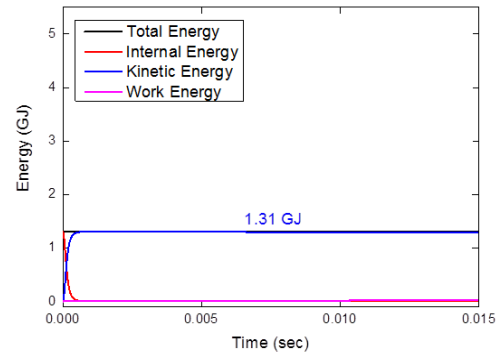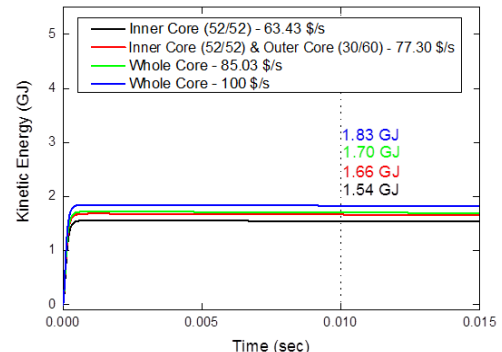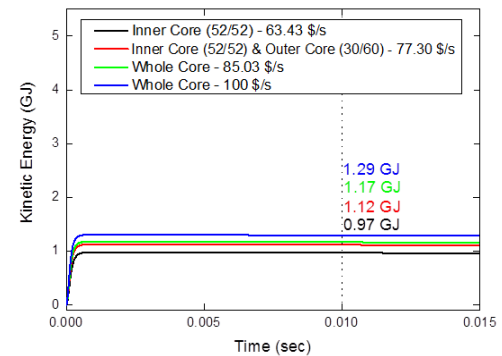

Fig. 19. Energy distributions during 0.015 seconds after the explosion with Doppler effect in PGSFR when whole cores were melted (conservatively 100 $/s).
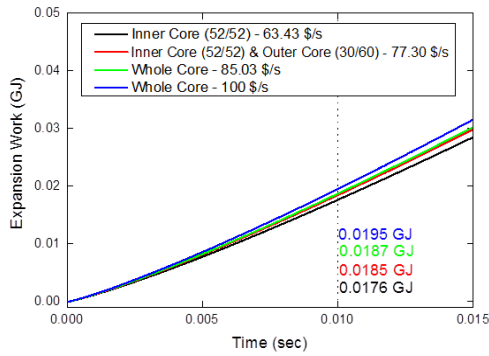

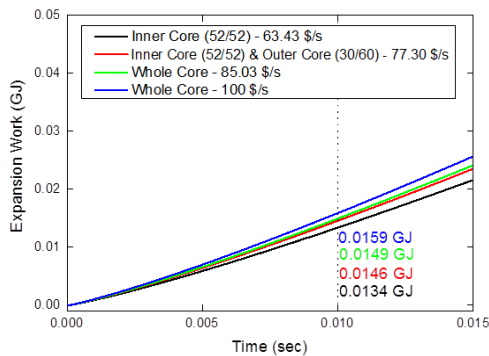(a) Without Doppler effect

(b) With Doppler effect

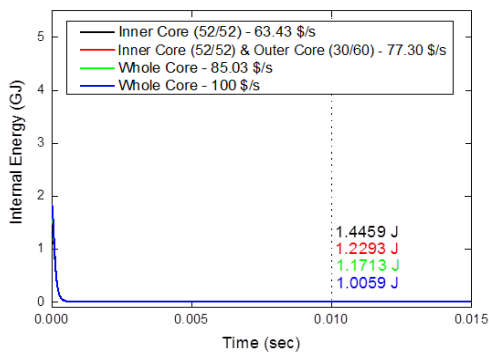Fig. 20. Kinetic energy in PGSFR according to the degree of core melting.
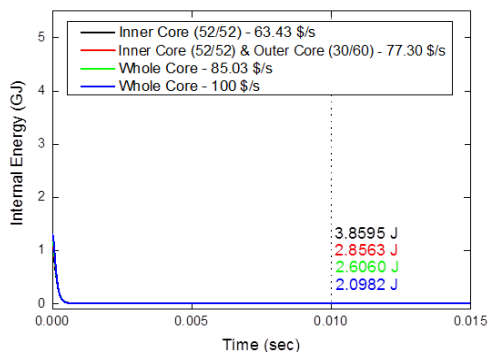
(a) Without Doppler effect

(b) With Doppler effect

Fig. 21. Expansion work in PGSFR according to the degree of core melting.

(a) Without Doppler effect

(b) With Doppler effect

Fig. 22. Internal energy in PGSFR according to the degree of core melting.

Fig. 20 and Fig. 21 show the kinetic energy and expansion work in PGSFR according to the degree of

core melting. The more the degree of core melting is, the larger the kinetic energy and expansion work are without and with Doppler effect. Fig. 22 shows the internal energy in PGSFR according to the degree of core melting. The more the degree of core melting is, the smaller the internal energy is.

4. Conclusions

A numerical analysis is conducted to estimate the energy release, pressure behavior and core expansion behavior induced by CDA of PGSFR using CDA-ER and CDA-CEME codes.

Conservatively, the calculated results of energy release and pressure behavior induced by CDA without Doppler effect in PGSFR when whole cores were melted (100 $/s) were 7.80 GJ and 4.79 GPa, respectively. With Doppler effect, the analyzed maximum energy release and pressure were 6.65 GJ and 3.39 GPa, respectively.

The calculated results of the core expansion behavior during 0.015 seconds after the explosion without Doppler effect in PGSFR when whole cores were melted (100 $/s) were as follows: The total energy is calculated to be 1.85 GJ. At 0.01 s, the kinetic energy of the sodium is 1.83 GJ, while the expansion work and internal energy of the bubble are 19.5 MJ and 1.01 J, respectively. With Doppler effect, the total energy is calculated to be 1.31 GJ. At 0.01 s, the kinetic energy of the sodium is 1.29 GJ, while the expansion work and internal energy of the bubble are 15.9 MJ and 2.10 J, respectively.

Though this scoping analysis is calculated to very conservative method and has a large difference from the point of view of a practical approach, it seems to give basic insight into the worst case in CDA of PGSFR.

REFERENCES

[1] IAEA Safety Standards Series No. NS-G-2.15, STI/PUB/1376, Severe Accident Management Programmes for Nuclear Power Plants - Safety Guide, Vienna, 2009.
[2] http://www.nrc.gov.
[3] IRSN-2007/83, Research and Development with regard to Severe Accidents in Pressurised Water Reactors: Summary and Outlook, 2007.
[4] T. G. Theofanous, C. R. Bell, An Assessment of CRBR Core Disruptive Accident Energetics (NUREG/CR-3224), Los Alamos, New Mexico, 1984.
[5] A. J. Brunett, A Methodology for Analyzing the Consequences of Accidents in Sodium-Cooled Fast Reactors, A Master's Thesis, The Ohio State University, 2010.
[6] A. E. Dubberley, C. E. Boardman, A. J. Lipps, T. Wu, "S-PRISM Metal Core Margins to Severe Core Damage," Proceedings of the 8th International Conference on Nuclear Engineering (ICONE-8), April 2-6, 2000, Baltimore, USA.
[7] H. A. Bethe, J. H. Tait, An Estimate of the Order of Magnitude of the Explosion when the Core of a Fast Reactor Collapses, UKAEA-RHM, Vol. 56, 1956.
[8] S. H. Kang, H. Y. Jeong, Scoping Analysis on Core Explosion and Energy Release of Liquid Metal Fast Reactor

during Core Meltdown Severe Accident, International Congress on the Advances in Nuclear Power Plants (ICAPP 2013), April 14-18, 2013, Jeju Island, Korea.

[9] 임재용, PGSFR 안전해석 입력 자료 2 차 – 원자로설계, SFR-IOC-R/S-14-008, 20140626.

[10] 한인수, PGSFR 안전해석용 기계분야 입력자료, SFR-IOC-M/S-14-008, 20140428.

[11] 이민재, PGSFR 중대사고 안전해석 노심분야 입력자료, SFR-IOC-R/S-14-009, 20140731.

[12] S. H. Kang, K. S. Ha, Numerical Study on Code Development to Analyze Energy Release during Core Disruptive Accident of Sodium Cooled Fast Reactor, KAERI/TR-5003/2013.

[13] R. H. Cole, Underwater Explosions, Dover Publications Inc., 1965.

[14] G. S. Yeom, Two-dimensional Two-fluid Two-phase Analysis of Underwater Shock Wave, 2005.

[15] L. E. Kinsler, A. E. Frey, Fundamentals of Acoustics, Second Ed., John Wiley & Sons, New York, USA, 1962.

[16] S. H. Kang, K. S. Ha, Analysis of Core Expansion and Energy Behavior during Severe Accident of Sodium Cooled Fast Reactor, Transactions of the Korean Nuclear Society Spring Meeting, May 30-31, 2013, Gwangju, Korea.